論文の内容の要旨

Size-Controlled Metal Nanoparticles on SBA-15 with Immobilized Ionic Liquid: Synthesis, Structural Properties and Catalytic Performances

（イオン液体を固定化したSBA-15上のサイズ制御された金属ナノ粒子：合成、構造及び触媒活性に関する研究）

クスマワティ. エッティ ヌルリィア

Introduction

Metal nanoparticles (MNPs) have attracted tremendous attention as reflected by the large number of publications especially in the field of catalysis as heterogeneous catalysts. Most of the syntheses procedures of these metal nanoparticles are based on wet methods by using soluble metallic precursors loaded on solid supports. It is very important to develop effective methods for size- and shape-controlled syntheses of MNPs, since it can result in modulating of their physical and chemical properties, and affects the catalytic performance of the catalyst. Many approaches have been adopted by controlling the concentration of the ratio between reducing agent and metal precursor, pH of solution, synthesis temperature, and the presence of stabilizing agent such as polymers, surfactants and ionic liquids (ILs). The use of stabilizers or capping agents is the most efficient way to control the nucleation and growth of the nanoparticles to avoid it from agglomeration. Although successive studies have been done, most of the approaches are limited in the colloidal system and only few have been reported on solid supports, especially inside porous materials. The limited number of researches on such studies may be due to the formation of large particles inside pores. These large particles give pore-blocking effect which results in the decrease of the catalytic performances. Hence, the development and well investigation on the size-controlled syntheses of MNPs inside porous materials, remain a challenge.

In order to overcome these limitations, in my doctoral study I have developed heterogeneous catalysts based on supported MNPs with a controlled size on mesoporous silica. This work demonstrates the synthetic procedure for immobilization and size-controlled syntheses of MNPs inside porous SBA-15 in the presence of ILs using $NaBH_4$ as the reducing agent. The resulting materials were characterized to study their structural properties and their catalytic performance was tested to investigate its activity and reusability. The following subjects have been studied; size-controlled gold nanoparticles prepared from immobilized gold ion-containing IL on SBA-15, size-dependence of AuNPs in the reduction of *p*-nitrophenol (PNP), immobilization of various metal (Pd, Au, Cu, Ru and Pt) nanoparticles as active and reusable catalysts, and room temperature Suzuki-Miyaura coupling reaction catalyzed by palladium nanoparticles.

1. Size controlled gold nanoparticles prepared from immobilized gold ion-containing ionic liquid on SBA-15

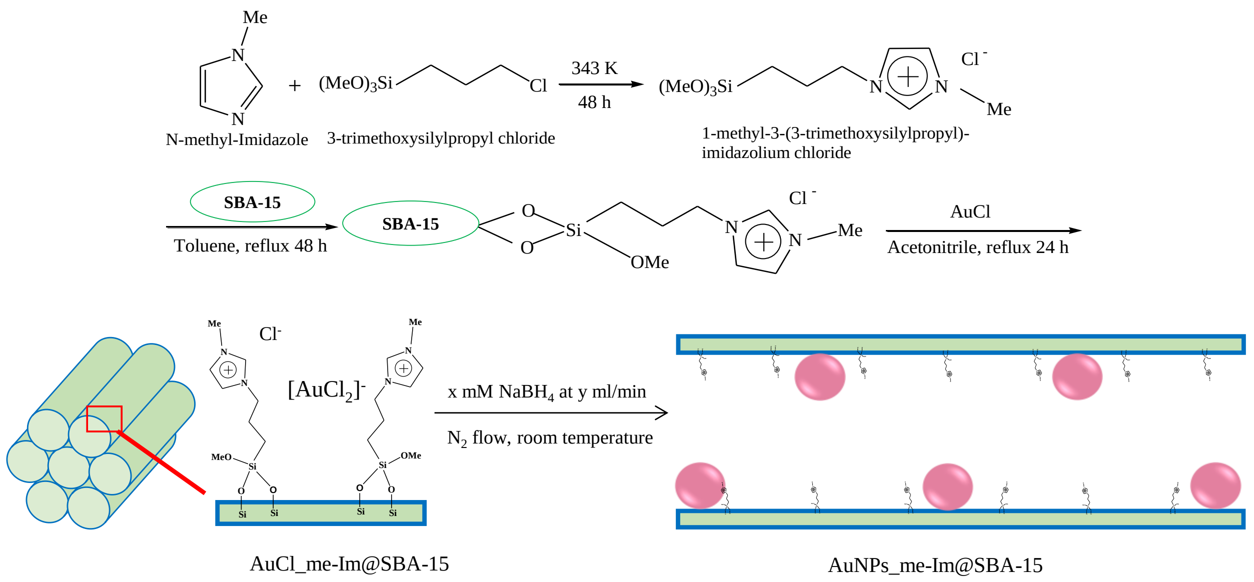

Scheme 1. Preparation steps for the syntheses of AuNPs_me-Im@SBA-15.

A series of gold nanoparticles (AuNPs) with controlled size were prepared from immobilized gold-containing ionic liquid on SBA-15 (AuCl_me-Im@SBA-15) at room temperature (20 °C). AuNPs size and shape could be controlled inside porous SBA-15 in the presence of immobilized 1-methyl-3-(3-trimethoxy-silylpropyl)-imidazolium chloride by controlling the concentration and feed rate of the reducing agent $NaBH_4$ (Scheme 1). TEM observations were used to study the effects of different concentration and feed rate of $NaBH_4$ solution on the size distribution of Au nanoparticles (Fig.1 and 2).

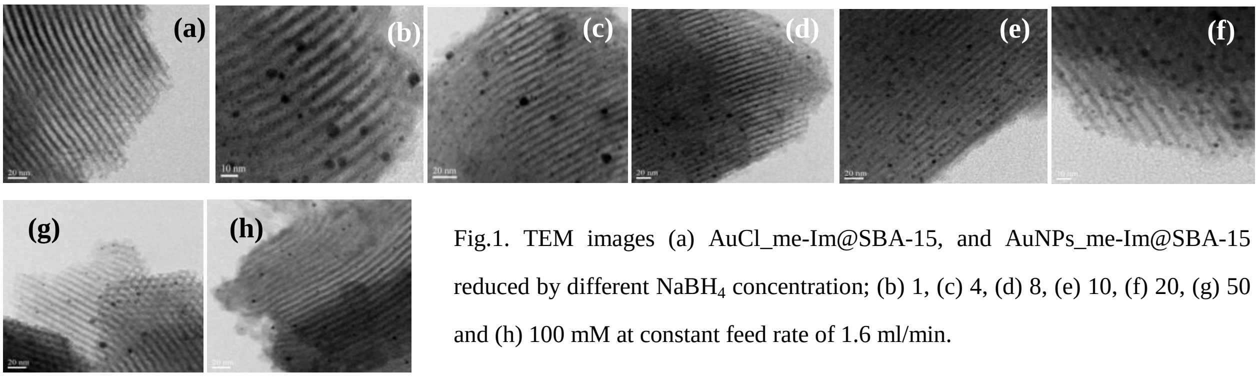

Fig.1. TEM images (a) AuCl_me-Im@SBA-15, and AuNPs_me-Im@SBA-15 reduced by different $NaBH_4$ concentration; (b) 1, (c) 4, (d) 8, (e) 10, (f) 20, (g) 50 and (h) 100 mM at constant feed rate of 1.6 ml/min.

The number of large NPs decreased and that of small NPs increased as the concentration of $NaBH_4$ increased resulting in the decrease of the average NPs size from 3.4 to 2.1 nm. Increasing the concentration of $NaBH_4$ resulting in the increase of pH of the solution from 4.51 at 1 mM to 9.74 at 100 mM. At higher concentration of $NaBH_4$, the Cl^- ions were replaced by OH^- ions to a larger extent. These results were confirmed from XPS analysis for Cl 2p region which shows the disappearances of both Cl $2p_{1/2}$ and Cl $2p_{3/2}$ peaks at higher $NaBH_4$ concentration. It seems that these adsorbed OH^- on AuNPs surface might help to avoid agglomeration due to electrostatic stabilization by forming a protective layer. On the other hand, by slowing the feed rate from

1.6 to 0.2 ml/min with 4 mM of $NaBH_4$, the average NPs size decreased from 2.7 to 1.6 nm (Fig.2). But further deceleration from 0.2 to 0.04 ml/min resulted in the increasing average NPs size from 1.6 to 2.7 nm and transformed the shape from spherical to capsule-like NPs. This trend can be understood by the relation between the reduction of gold precursor and the growth rates of NPs in different conditions.

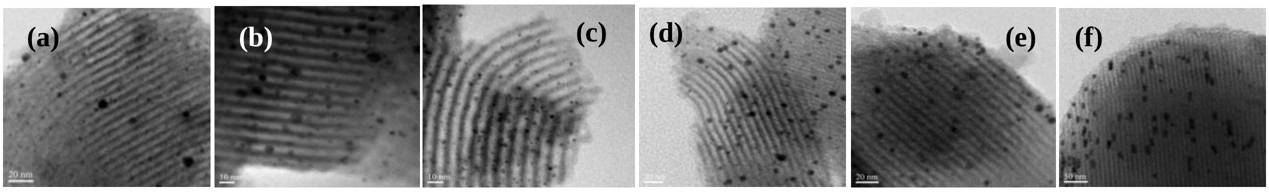

Fig.2. TEM images of AuNPs_me-Im@SBA-15 reduced by 4 mM of $NaBH_4$ at different feed rate of (a) 1.6, (b) 0.4, (c) 0.2, (d) 0.1, (e) 0.06 and (f) 0.04 ml/min.

2. Size-dependence of gold nanoparticles in the reduction of *p*-nitrophenol

To investigate the difference in catalytic performance of supported AuNPs catalysts with different size, three different sizes of Au NPs; 1.6, 2.4 and 2.7 nm, were selected for the reaction. The cuvette with 3 ml mixture of Au:PNP:$NaBH_4$ = 1:10:500 was quickly inserted in UV-vis spectrometer and the reaction progress was monitored at 1 min interval under stirring at room temperature (20 °C). The average apparent reaction rate constant with error (k_{app} ± error) was calculated by measuring the absorbance (A) of PNP at 400 nm and plotting $\ln(C_t/C_0)$ versus reaction time (t) from three experiments using fresh catalyst. The ratios of PNP concentrations (C_t) to the initial concentration (C_0) were given by the relative intensity of the respective absorbance (A_t/A_0) at 400 nm. The negative slope of the best fit gave the pseudo-first-order rate constant and the average k_{app} values were summarized in Table 1.

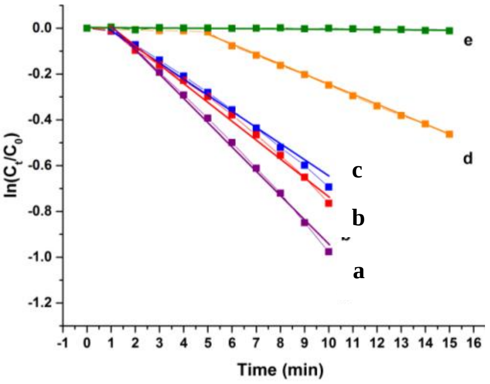

Fig. 3. The relationship between $\ln(C_t/C_0)$ and reaction time (t) of different prepared Au NPs size: (a) 1.6 nm, (b) 2.4 nm, (c) 2.7 nm, (d) AuCl_me-Im@SBA-15, and (e) Au/SBA-15.

The results in Fig. 3 show that AuNPs(1.6 nm)_me-Im @SBA-15 gave the highest kinetic constant as compared to that of AuNPs with larger size (Table 1). It means that the smallest NPs have higher catalytic activity compared to larger particles. In addition, small particles could minimize the pore-blocking that can be caused by large NPs on porous materials, facilitating the reactant to reach more particles (active sites) deeper inside porous channels, resulting in better catalytic performance. This pore-blocking effect gave longer induction period for larger NPs as shown in the reaction by Au/SBA-15 (5.6 nm) resulting in the lowest k_{app} value. In the case of reduction by AuCl_me-Im@SBA- 15 catalyst, the induction period occurred from t = 0–5 min suggesting that the reduction of PNP cannot proceed before the complete reduction of $AuCl_2^-$ anions to AuNPs.

Table 1. The average apparent rate constants of the prepared AuNP catalysts in the reduction of PNP.

Sample:	Catalyst	k_{app} x10^{-3} ($s^{-1}mmol^{-1}$)
a.	AuNPs(1.6 nm)_me-Im@SBA-15	4.70 ± 0.07
b.	AuNPs(2.4 nm)_me-Im@ SBA-15	4.10 ± 0.04
c.	AuNPs(2.7 nm)_me-Im@ SBA-15	3.80 ± 0.06
d.	AuCl_me-Im@ SBA-15	1.80 ± 0.05
e.	Au/ SBA-15 (5.6 nm)	0.08 ± 0.00

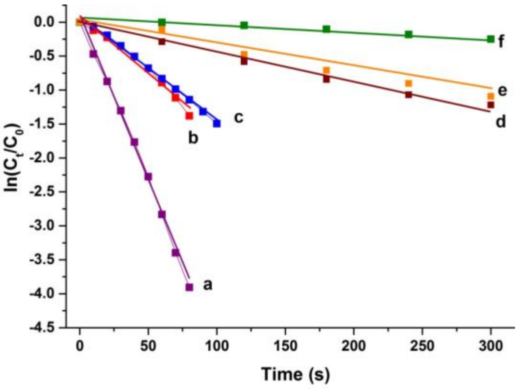

Fig. 4. The relationship between ln(C_t/C_0) and reaction time (t) different prepared MNPs catalysts.

Table 2. The average apparent rate constants of the prepared MNP catalysts in the reduction of PNP.

Sample:	Catalyst	k_{app} x10^{-3} ($s^{-1}mmol^{-1}$)
a.	PdNPs (2.4 nm)	113.50
b.	PdNPs (3.4 nm)	44.04
c.	AuNPs (2.0 nm)	16.0
d.	PtNPs (2.1 nm)	1.56
e.	RuNPs (2.7 nm)	5.46
f.	CuNPs (2.9 nm)	1.66

3. Immobilized metal nanoparticles (Pd, Au, Cu, Ru and Pt) as active and reusable catalysts

Based on the above mentioned findings, various metal nanoparticles (Au, Pd, Cu, Ru and Pt) were successfully prepared from immobilized metal ions containing ionic liquids on SBA-15 using 100 mM $NaBH_4$ solution at 0.2 ml/min. The effects of different metal NPs with average sizes of 2–4 nm in *p*-nitrophenol reduction have been studied. In addition, PdNPs containing different alkyl-chain length ionic liquids were prepared in order to study its effects on the NPs size as well as catalytic performance. All prepared materials were characterized by TEM, XAFS, FTIR, XPS, solid state NMR, and N_2 adsorption-desorption isotherm. Characterization of the catalysts revealed that the metal atom was coordinated by chloride atoms forming metal chloride complex anion before reduced to MNPs. The prepared catalysts were found active and reusable for transfer hydrogenation reaction of *p*-nitrophenol at room temperature (25 °C) with highly specificity to convert into *p*-aminophenol (PAP). The order of rate constant for fresh catalyst is PdNPs(2.4 nm) > PdNPs(3.4 nm) > Au > Ru > Pt > Cu.

4. Room temperature Suzuki-Miyaura coupling reaction catalyzed by Pd nanoparticles

Immobilized palladium nanoparticle on ionic liquid functionalized SBA-15 (PdNPs(2.4 nm)_me-Im @SBA-15) has been investigated as ligand-free catalyst for Suzuki-Miyaura cross-coupling reaction at room temperature. The catalyst was found active for the coupling reaction between aryl iodides (bromides) and phenylboronic acid in aqueous solution under air. The catalyst was reusable at least for four recycle processes without significant loss in activity with simple procedure.

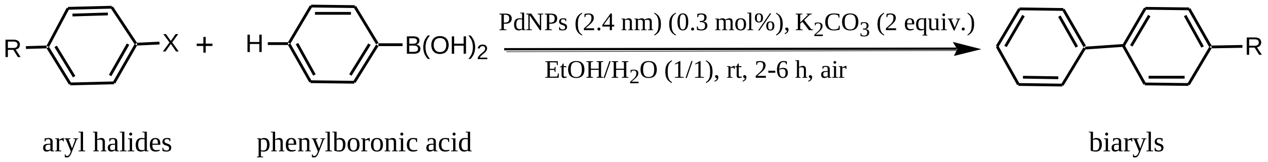

Conclusions

AuNPs catalysts with controlled size have successfully been prepared from immobilized gold chloride on ionic liquid functionalized SBA-15 by varying the concentration and feed rate of $NaBH_4$ and the prepared AuNPs(1.6 nm) exhibited the best catalytic performance with the highest rate constant. Various metal nanoparticles were also successfully prepared on SBA-15 as active and reusable catalysts in the reduction of *p*-nitrophenol. In addition, PdNPs_me-Im@SBA-15 was found active and reusable for Suzuki-Miyaura coupling reaction at room temperature. All the prepared catalysts were characterized to study their structural properties.